Exploring the mechanisms of fine ash generation: methods of ash characterisation

Emma J. Liu, Katharine V. Cashman, & Alison C. Rust

Department of Earth Sciences, University of Bristol, Wills Memorial Building, Bristol, BS8 1RJ

Introduction

The disruption during the recent Icelandic eruptions of Eyjafjallajokull (2010) and Grimsvotn (2011) was caused by the large volume of fine ash produced during the early phreatomagmatic phases of both eruptions. This highlighted gaps in our knowledge regarding the fragmentation mechanisms that generate volcanic ash in basaltic systems, particularly the role of magma-water interactions in controlling the size and shape of the resulting pyroclasts.

By quantifying the variation in morphology and componentry with grain size, and comparing this relationship to the corresponding vesicle textures, we explore the potential role of bubbles in phreatomagmatic fragmentation.

Grainsize Distributions for Mafic Eruptions

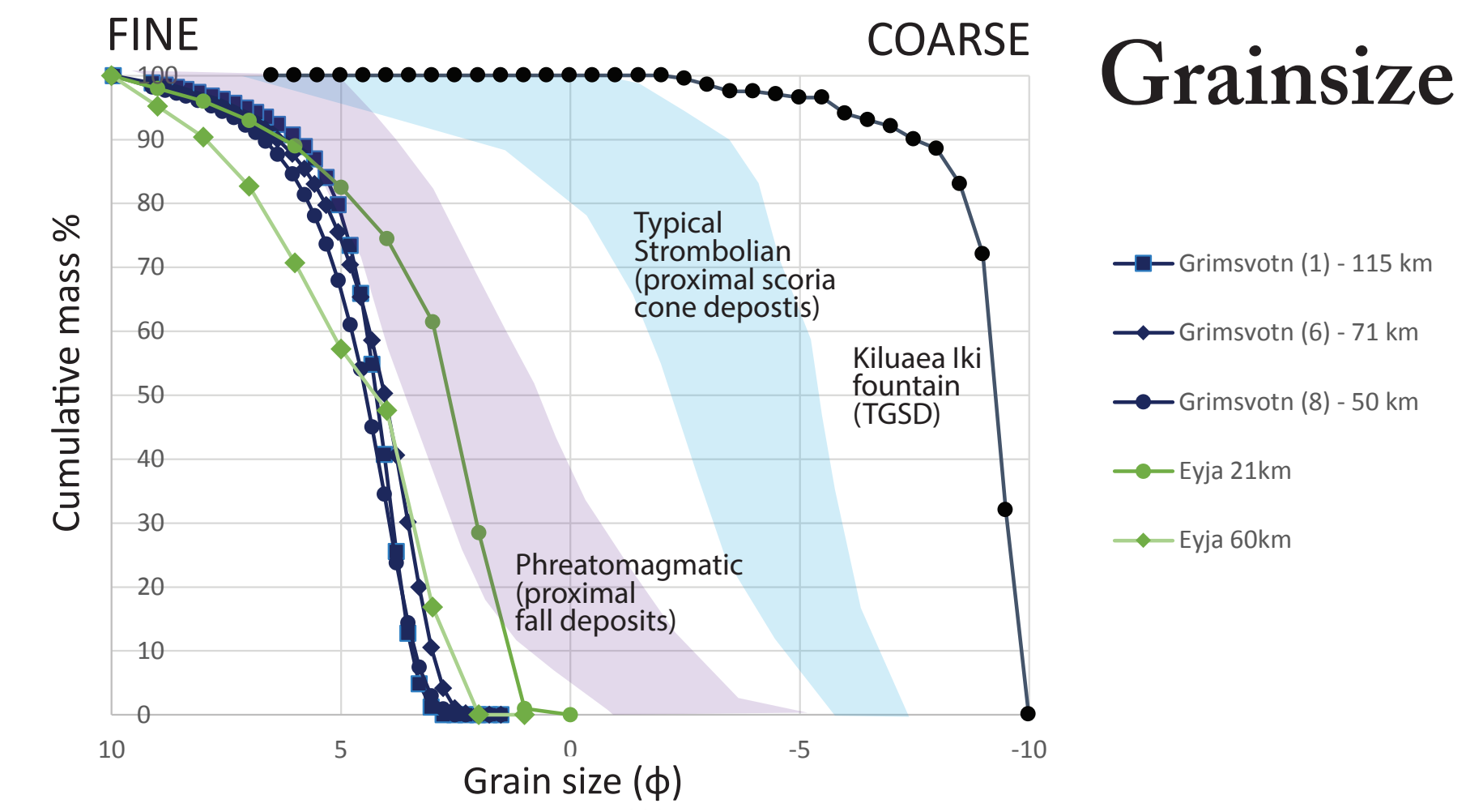

Fig. 1: Compilation of grainsize distributions for mafic eruptions (data from Houghton and Hackett, 1983; Houghton and Schminke, 1989; Houghton and Nairn, 1991; Nemeth and Cronin, 2011; Gudmundsson et al., 2012; Parfitt, Olsson et al. 2013)

Mafic eruptions involving magma-water interactions typically produce finer grained deposits than equivalent dry eruptions.

The 2011 Grimsvotn eruption generated a large proportion of fine ash.

Making Measurements

Shape parameters provide numerical measures of particle shape. They are typically non-dimensional, formed from ratios of different measures of particle size (e.g. perimeter, feret diameter, convex hull).

Understanding how shape parameters translate to physical properties is key to their use as a tool in ash characterisation.

Image aquisition

Resolution: critical pixel density >750 pixels per particle
Sample size: >1000-2000 particles statistically significant

Instrument: we find fundamental differences in the results obtained between cross-section and projected view techniques

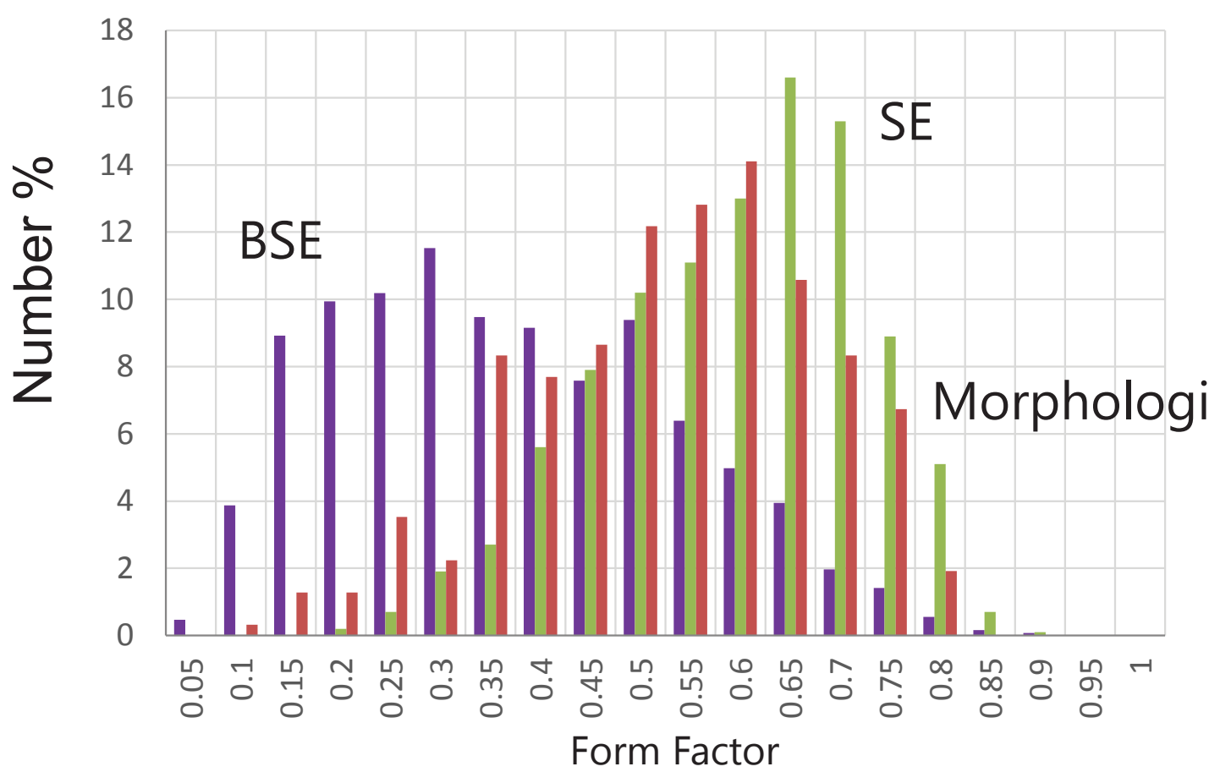

Fig. 2: Comparison of results for 'Form Factor' obtained by backscattered electron BSE-SEM (cross-sectional), secondary electron SE-SEM (projected), and Morphologi optical particle analyser (projected).

Shape Parameter Selection

Shape parameters are sensitive to different aspects of particle morphology.

We used cluster analysis to explore the relationships between commonly-used shape parameters (Fig. 3). The clustergram structure is independent of the morphology of the particles analysed.

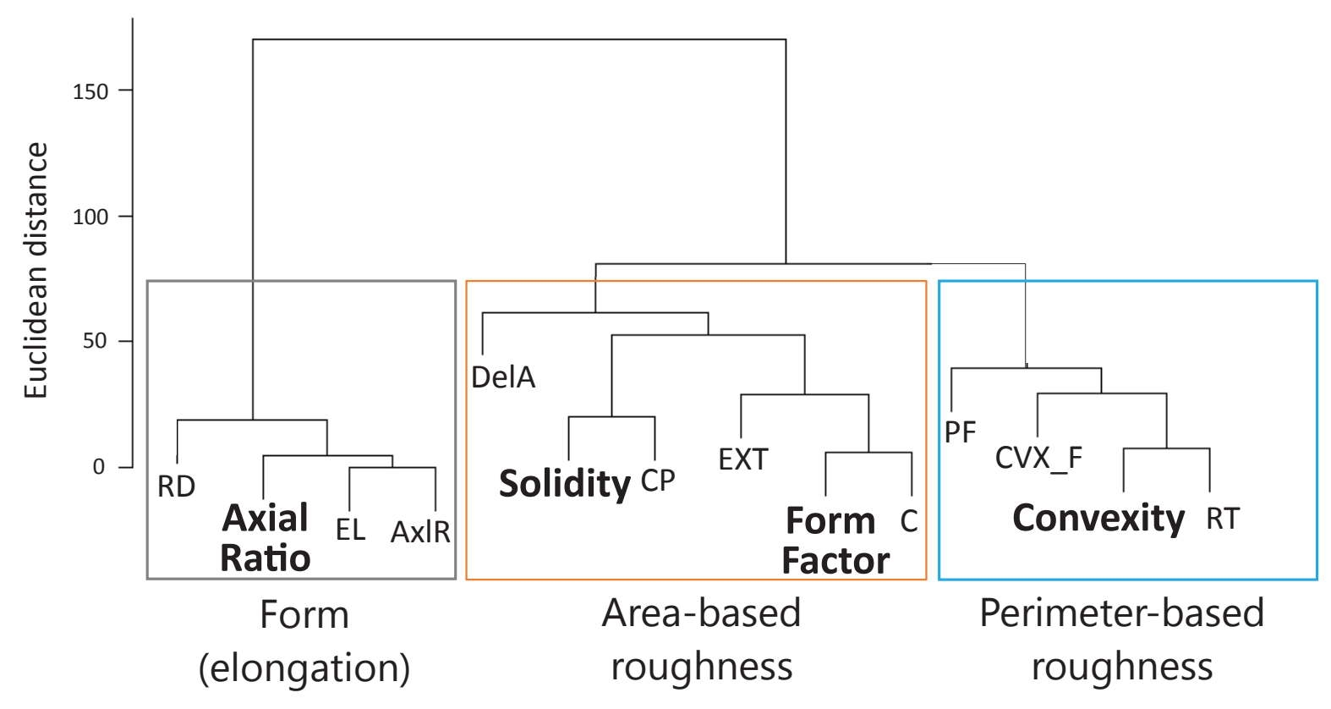

Fig. 3

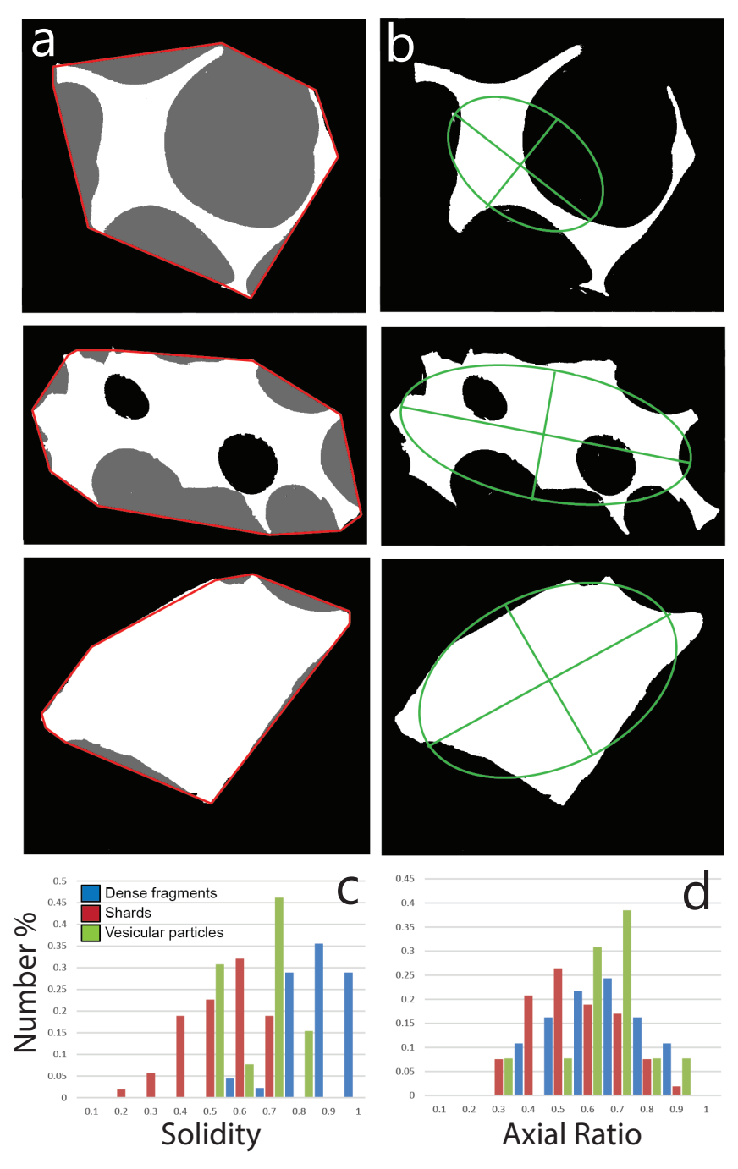

Parameters sensitive to the convex hull (perimeter of an elastic band stretched around a particle) are very effective at discriminating based on vesicularity:

- (a) Shards: particle-scale (morphological) concavities. Low solidity.
- (b) Vesicular grains: many small (textural) concavities. Low convexity.
- (c) Dense fragments: few concavities High convexity and solidity.

Parameters that compare to an equivalent-area reference shape (e.g. circle) and axial ratio are poor discriminators of vesicularity.

Fig. 4: Variation in (a) convex hull and (b) best-fit ellipse for shards, vesicular grains and dense fragments; example distributions of (c) solidity and (d) axial ratio, for subsample of Grimsvotn ash (4 φ size)

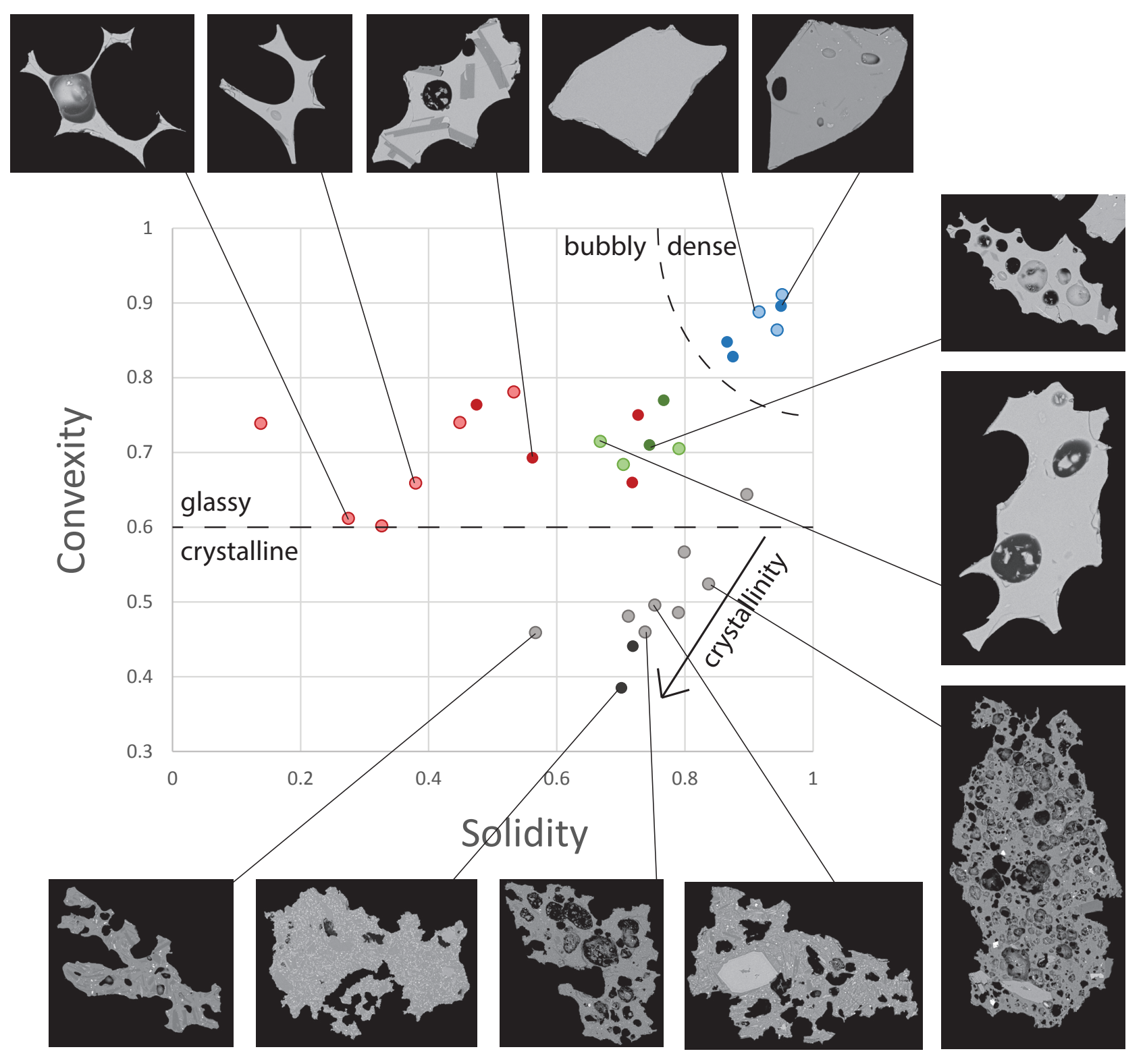

Fig. 9

What about crystals?

A microlitic groundmass changes the bubble texture from smooth isolated spheres to irregular and convoluted. Interconnectivity also increases.

The effect of this is to significantly increase convexity (perimeter-based roughness), with relatively little increase in solidity (excess area). Scattered crystals in a glassy matrix are indistinguishable from crystal-free glass, however, as the crystals do not influence the bubble texture.

2011 Grimsvotn eruption, Iceland

SEM Analysis

We analysed ash samples collected during the first 24 hours of the 2011 eruption, from sites between 30 and 115 km from the vent. Samples were sieved and mounted for SEM analysis as individual size fractions.

Grimsvotn ash is morphologically heterogeneous. Particles can be classified into two main components, which can be effectively discriminated using shape parameters sensitive to the 'convex hull'

(1) dense fragments (blocky, fracture-bounded)
(2) bubbly shards and vesicular grains (irregular, vesicle-bounded)

$$\mathit{Concavity\ index}, CI = \sqrt{(1-\mathit{Solidity})^2 + (1-\mathit{Convexity})^2}$$

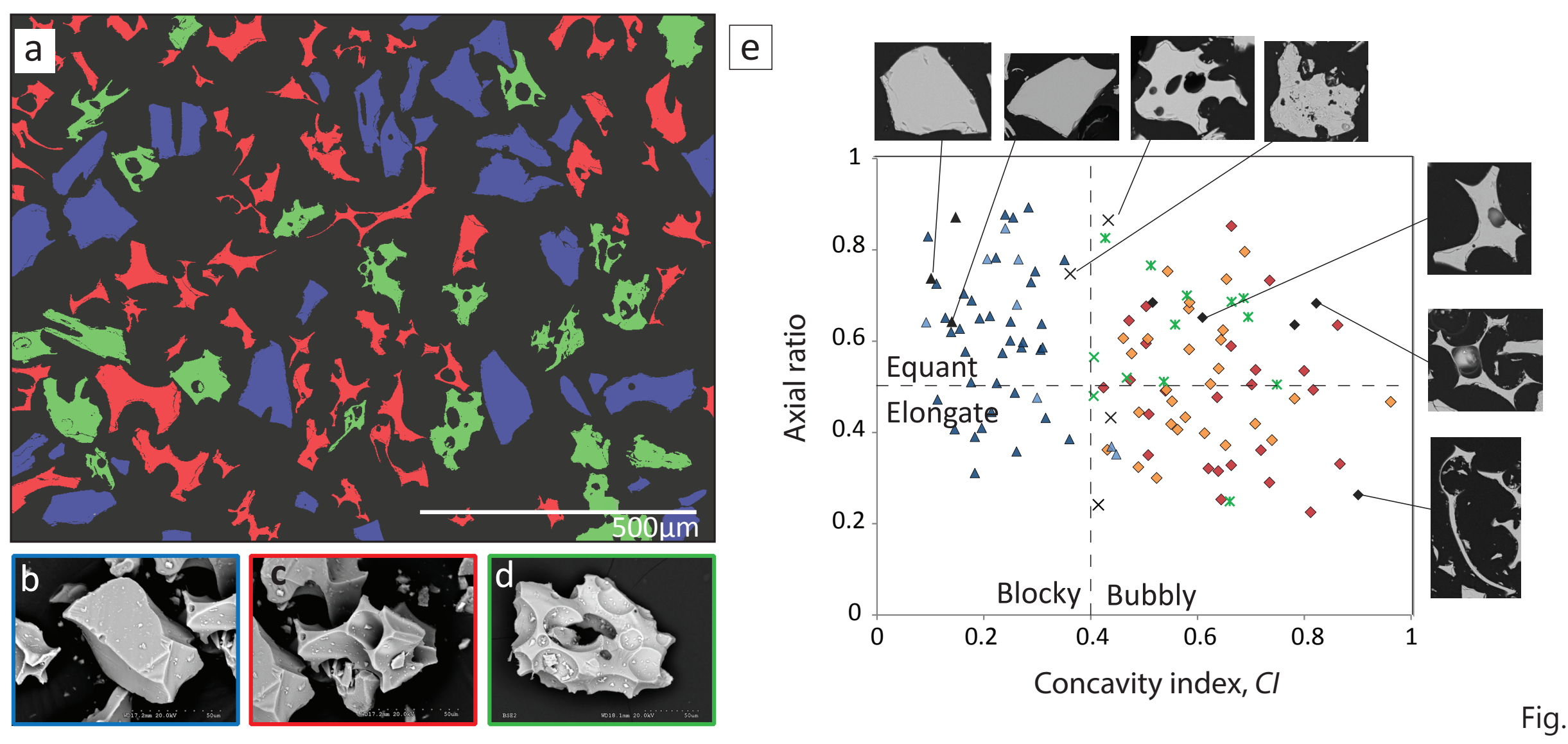

Fig. 7

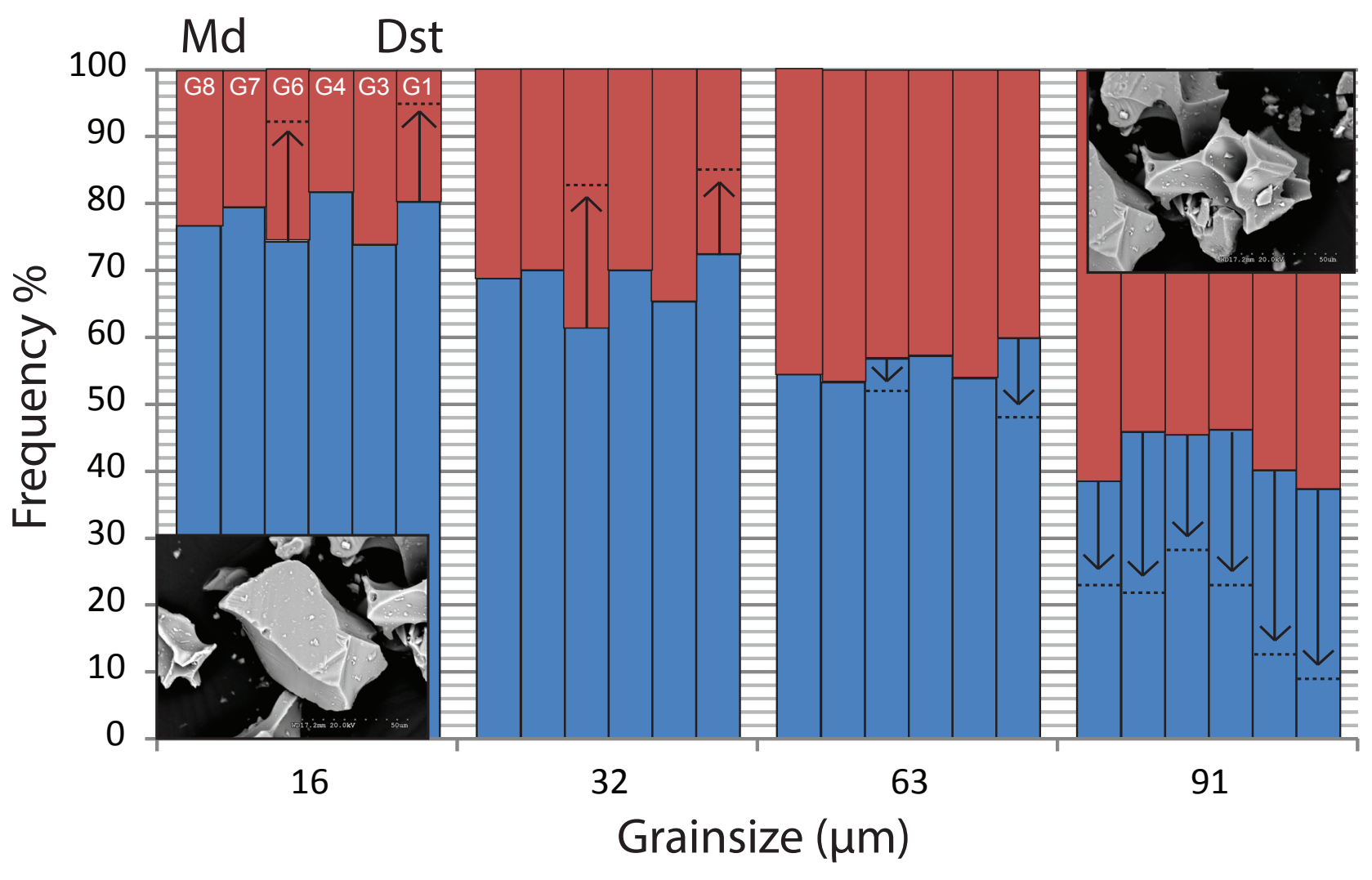

Fig. 8: Componentry as a function of grainsize. Automated componentry shown as shaded bars. Manual results illustrated by dotted lines.

Automated Componentry

Shape parameter measurements provide a rapid, reproducible and unbiased approach to estimate the proportions of different components within a sample. We observe good agreement between manual and automated results.

Our results demonstrate that the relative proportion of dense fragments to bubbly grains **increases** with **decreasing** size fraction.

Componentry measurements based on a single size fraction are not sufficient to characterise a deposit.

Fig.6: Sampling locations for the Grimsvotn ash

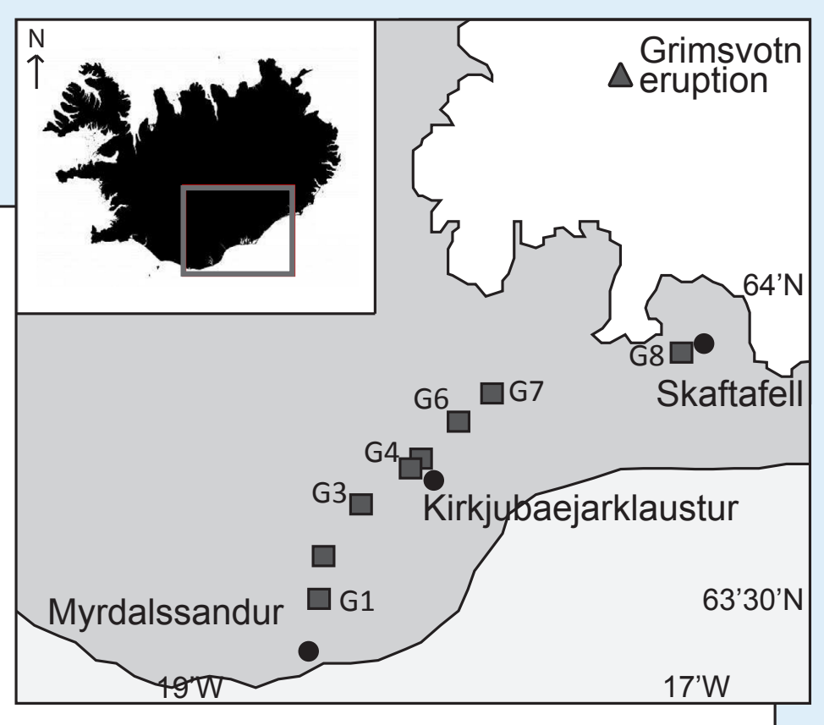

Linking external morphology to internal texture

We measured the distribution of 2D vesicle diameters from those grains where >50% of the bubble wall is preserved (solid black line).

We observe a systematic change in ash morphology (symbols) as the **particle size** approaches the **modal bubble size** (Fig. 9). Ash particles smaller than the mode of the bubble size distribution are dense, and represent the melt (glass) interstices between bubbles.

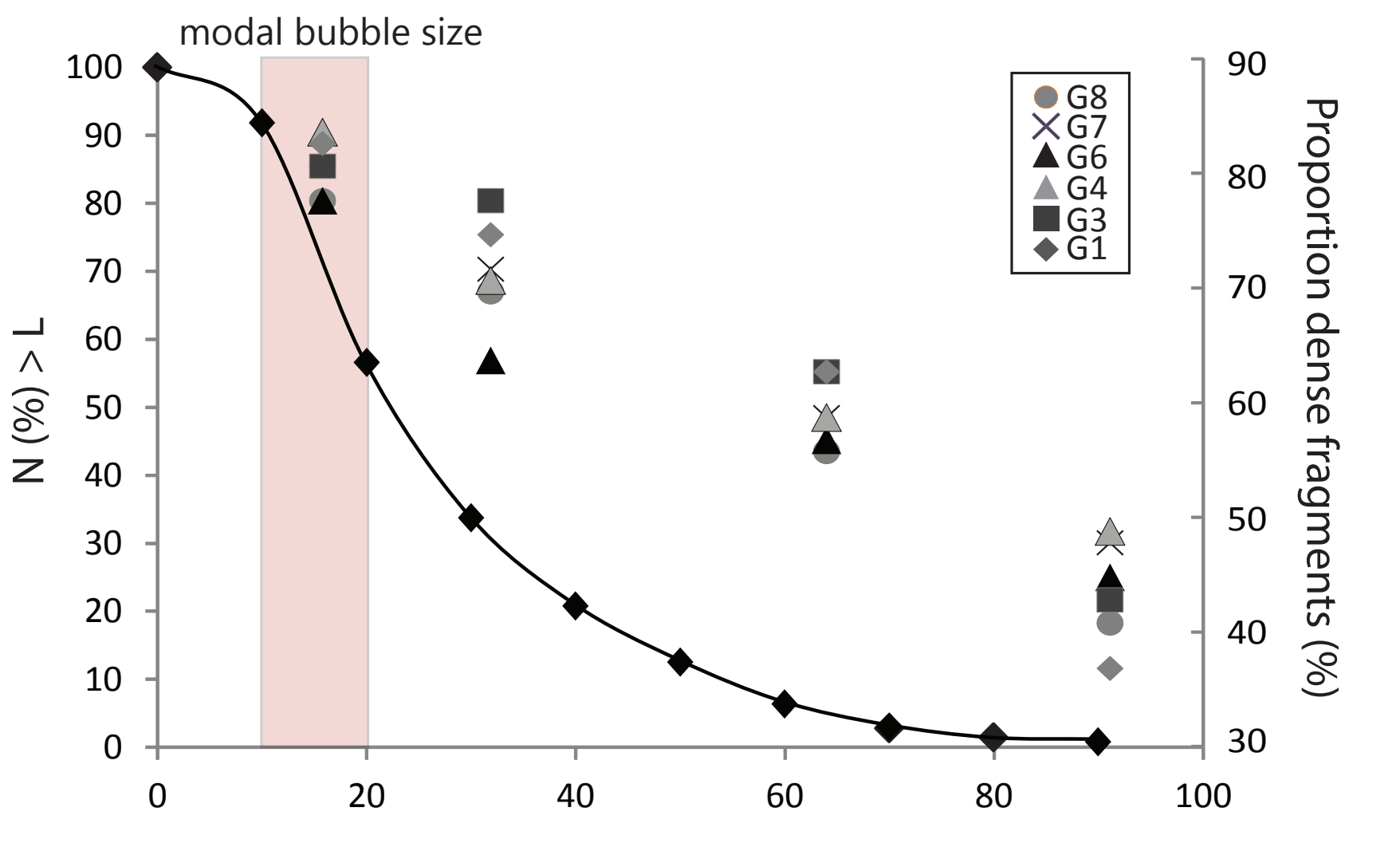

Fig. 9

Thermal Stresses in Phreatomagmatic Fragmentation

Grimsvotn ash shows evidence of both brittle and ductile fragmentation, often in the same clast (Fig. 10).

Differential cooling of magma interacting with water will develop residual thermal stresses in quenched pyroclasts, which may contribute to explosive thermal granulation of vesicular pyroclasts and amplify fine ash production.

The stress field around vesicles would provide a local control on brittle fracture propagation. The **shape and size of the resulting ash particles** would therefore be controlled by the **size and spatial distribution of bubbles** in the quenched primary pyroclasts.

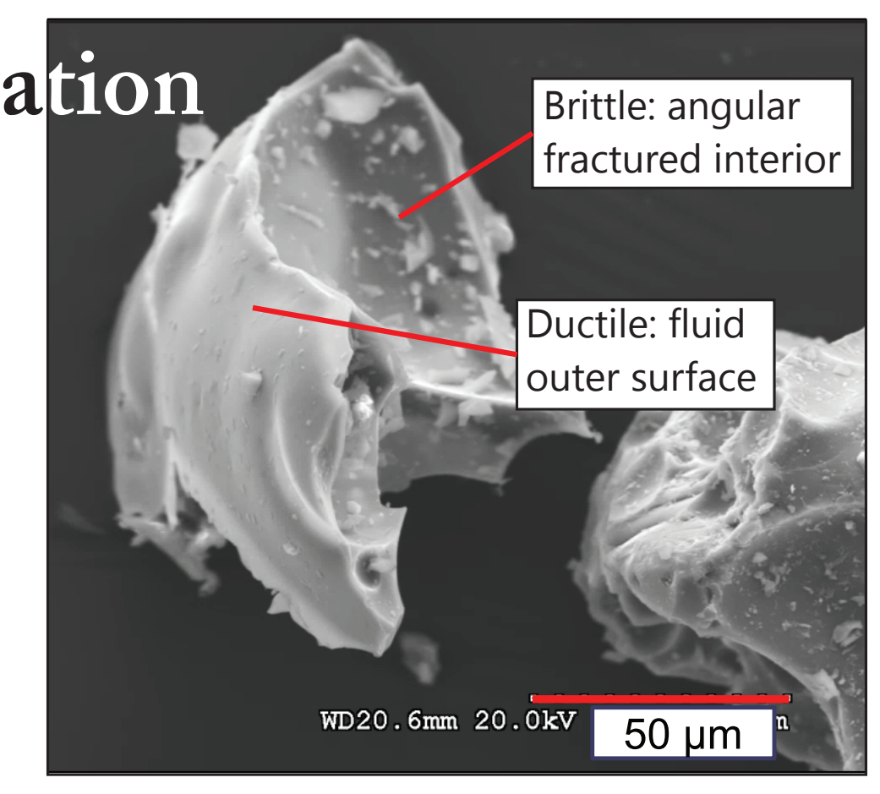

Fig. 10

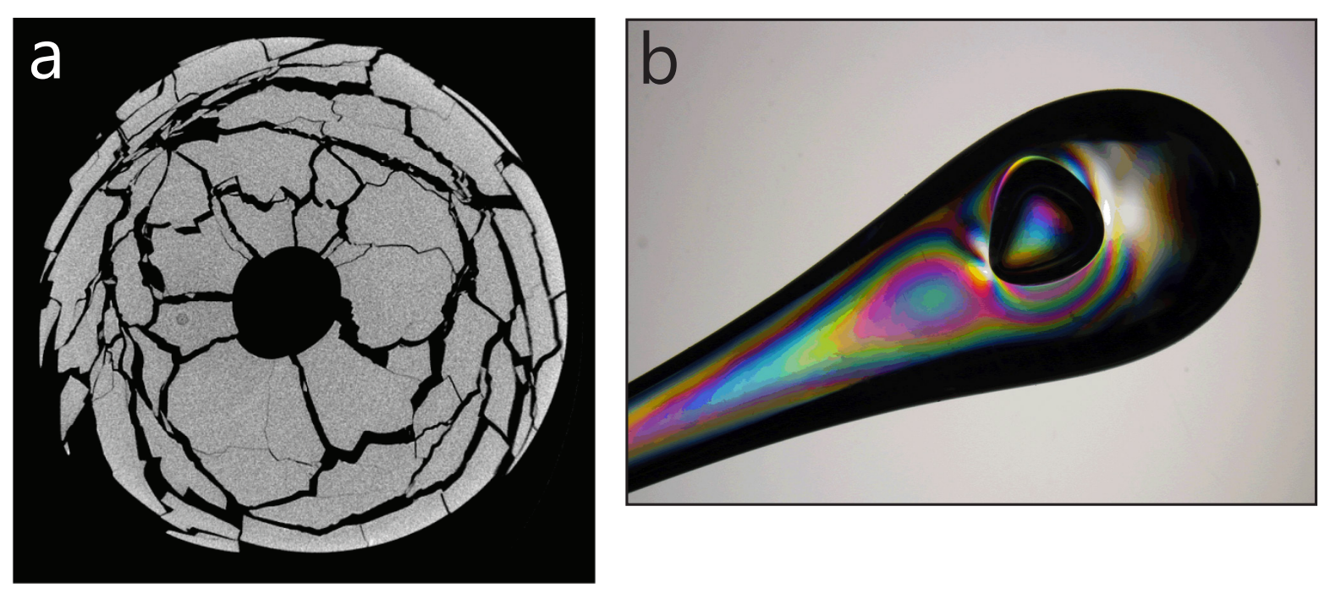

We have been exploring the role of residual stresses in phreatomagmatic fragmentation through the analogue of **Prince Ruperts Drops (PRDs)** - these quenched glass drops undergo explosive self-sustained fragmentation when broken and residual stresses are released.

Fragment morphology is spatially related to pre-existing bubbles in the glass, and share many of the shape and surface characteristics seen in Grimsvotn volcanic ash.

Fig.11: (a) Cross-section through fractured PRD, showing the influence of bubbles on fracture propagation; (b) residual stress field revealed by polarised filters.

Tephra Correlations - Deception Island, Antarctica

Componentry and textural measurements can aid correlations when chemical compositions are similar (e.g., single source volcano)

Combined with paleoenvironmental evidence, tephra stratigraphy in lake cores from Byers Peninsula, Antarctica, has constrained the timing of the Deception Island caldera collapse to ~4000 ka.

We measure an abrupt change in **crystallinity, morphology and composition** between T3 and T1/T2 layers. T3 is chemically similar to proximal deposits of the first ignimbrite phase of the Deception Island caldera collapse unit.

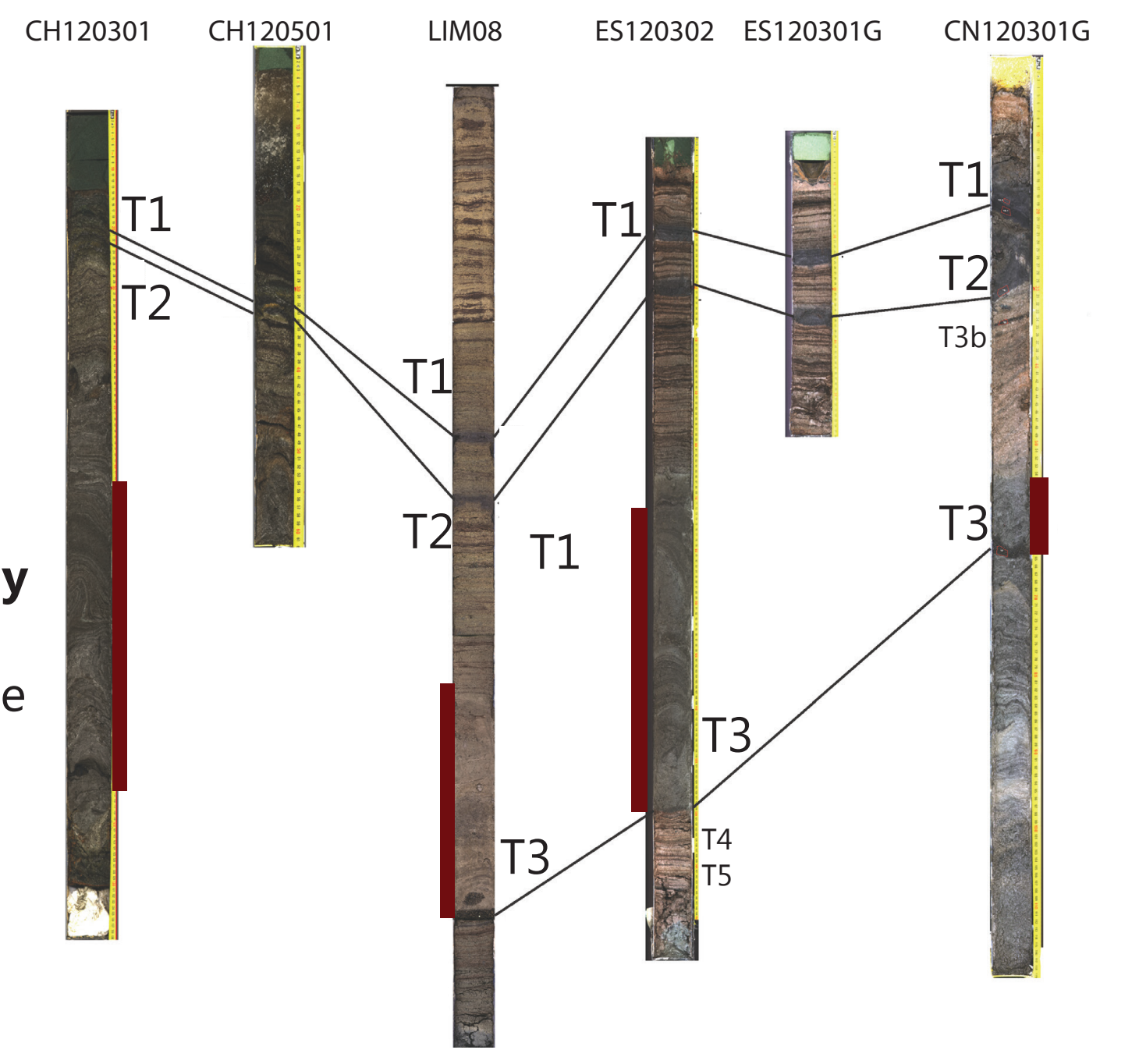

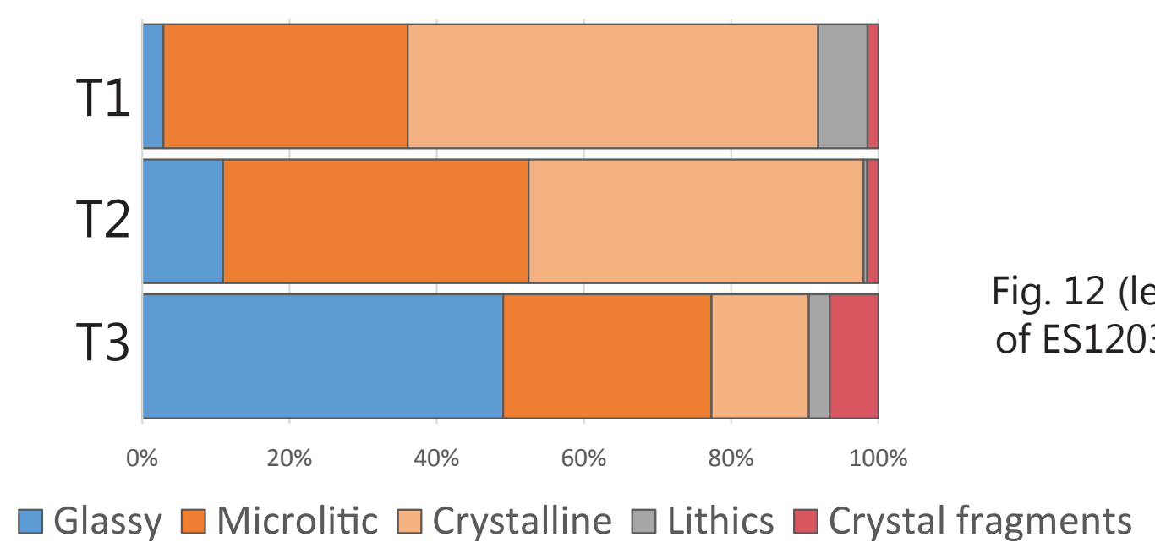

Fig. 12 (left): Relative proportions of components of different crystallinity within tephra layers of ES120302. Fig. 13 (above): Tephra chronological framework for Byers Peninsula, Antarctica, Red bars show syn-collapse sediment deformation.

In collaboration with the Holoantar paleoclimate group - Oliva, M., Giralt, S., Antoniades, D., & Geyer, A.